Available online at www.sciencedirect.com

ScienceDirect

Energy Procedia 126 (201709) 573–580

Energy Procedia

www.elsevier.com/locate/procedia

72nd Conference of the Italian Thermal Machines Engineering Association, ATI2017, 6-8 September 2017, Lecce, Italy

Potential of the Virtual Blade Model in the analysis of wind turbine wakes using wind tunnel blind tests

Alessandro Bianchini[a]*, Francesco Balduzzi[a], Domenico Gentiluomo[a], Giovanni Ferrara[a], Lorenzo Ferrari[b]

[a]*Dept. of Industrial Engineering (DIEF), Università degli Studi di Firenze, via di Santa Marta 3, Firenze 50139, Italy*
[b]*DESTEC, Università di Pisa, Largo Lucio Lazzarino, Pisa 56122, Italy*

Abstract

The present research frontier on wind turbine wake analysis is leading to a massive use of large-eddy simulations to completely solve the flow field surrounding the rotors; on the other hand, there is still room for lower-fidelity models with a more affordable computational cost to be used in extended optimization analyses, e.g. for a park layout definition. In this study, a customized version of the Virtual Blade Model (VBM) for ANSYS® FLUENT® is presented. The model allows a hybrid solution of the flow, in which the surrounding environment is simulated through a conventional RANS approach, while blades are replaced by a body force, calculated by a simplified version of the Blade Element Theory. The potential of the newly-customized VBM was evaluated by applying it to the famous NOWITECH-NORCOWE blind tests for horizontal axis wind turbines. Several test cases were analyzed and discussed including: 1) a single turbine; 2) an array of two turbines with one rotor working in the wake of the other one; 3) an array of two staggered rotors; 4) several configurations of rotors working in yawed-flow. The study proves that the VBM model can represent a valuable tool for the analysis of wind turbines wakes and of their interaction with near rotors.

Peer-review under responsibility of the scientific committee of the 72nd Conference of the Italian Thermal Machines Engineering Association

Keywords: wind turbine; VBM; wake; wind tunnel; CFD

1. Introduction

The leading role of wind energy in the world scenario is being consolidated in the last few years by all statistics.

* Corresponding author. Tel.: +39-055-275-8773; fax: +39-055-275-8755.
E-mail address: bianchini@vega.de.unifi.it

1876-6102
Peer-review under responsibility of the scientific committee of the 72nd Conference of the Italian Thermal Machines Engineering Association
10.1016/j.egypro.2017.08.212

A recent one [1] showed for example that 2015 was an unprecedented year for the wind industry, as annual installations crossed the 60 GW mark for the first time in history, with a cumulative annual market growth of more than 17%. The majority of this power is supplied by large rotors, often clustered into parks. In these installations, the mutual influence of wakes can have a tremendous impact on the turbine efficiency, reaching even 30-40% power losses and fatigue loads up to 80% larger if compared with turbines operating in undisturbed wind [2], with a notable decrease of both the expected revenue of the wind farm and the expected lifetime of the downwind turbines. Since experimental wake analyses of real-scale turbines are extremely expensive and often barely feasible, significant efforts have been made by researchers both in developing mathematical models for the wake description and in extensively using computational fluid dynamics (CFD) [3-4]. The computational cost of these approaches, especially if based on Large Eddy Simulations, is very high and often not compatible with extended optimization analyses typical of the industrial practice (e.g. for a park layout definition). Increasing interest is then devoted at defining simplified techniques for the analysis of wind turbine wakes [5], with particular focus on the far-wake interaction with downstream rotors. If well-known Reynolds-Averaged Navier-Stokes (RANS) CFD approaches represent a valuable trade-off in many applications [6], even more simplified models are being developed in case of multiple rotor analyses, in which a RANS CFD approach is used to solve the flow field everywhere in the domain except on the rotor blades, which are replaced by an equivalent energy extraction from the flow [7]. Upon comparison of these models [8], the authors recently suggested that the adaptation to wind turbines of the Virtual Blade Model (VBM) for ANSYS® FLUENT® may be particularly effective for wake studies. To this end, in the present study the potential of a customized and improved version of the VBM is then evaluated by applying it to the famous NOWITECH-NORCOWE blind tests to assess its potential in correctly reproducing the performance and wake shape of horizontal axis wind turbines in case of both aligned and skewed flow.

Nomenclature

c	local blade chord	[m]
c_D, c_L	drag, lift coefficient	[-]
Cp	power coefficient	[-]
D	turbine diameter	[m]
r, R	local radius, outer turbine radius	[m]
R^2	coefficient of determination	[-]
U	wind speed	[m/s]
y^+	dimensionless wall distance	[-]
Acronyms		
BEM	Blade Element Method	
CFD	Computational Fluid Dynamics	
RANS	Reynolds-Averaged Navier–Stokes	
TSR	Tip-Speed Ratio	
VBM	Virtual Blade Model	
Greek letters		
α	incidence angle	[rad]
γ	yaw angle	[deg]
ρ	fluid density	[kg/m^3]
Ω	turbine revolution speed	[rad/s]
Subscripts		
0	value at infinity	
x, y, z	directions of the reference axes	

2. Numerical techniques

The Virtual Blade Model (VBM) is a user-defined function proposed for the commercial solver ANSYS® FLUENT® (running with a RANS approach). This add-on was originally conceived to model the aerodynamics of propellers and helicopter rotors and it is still used extensively for these purposes, even in military applications [9]. Its application to HAWTs is, however, quite straightforward, even if still not so common (seen only in [7] and [11]).

2.1. Virtual Blade Model

The basic assumption of the VBM model is to replace the time-averaged aerodynamic effect of turbine blades (neither meshed nor modelled) with a momentum source term placed inside a rotor disk fluid zone with an area equal to the swept area of the turbine (Fig. 1(a)); no vorticity source can be introduced via the VBM model. This term is calculated with a classical BEM approach [10] that logically depends on the chord length, the angle of attack, and the tabulated aerodynamic coefficients of the airfoils. In this study, a customized version of the model was created, by incorporating a few modifications in the iteration procedure on the induction factor, following the experience collected by some of the authors in their in-house software HARDAR [12]. In addition, in order to improve the accuracy of the prediction of the turbine performance, the stall delay model by Du and Selig [13] was implemented within the VBM. This model, whose main equations for the 3D correction of 2D lift and drag coefficients are reported in Eqs. (1), (2), (3) and (4), in fact showed in the recent past a good accuracy for medium-size rotors with Selig-type airfoils [12]. A preliminary analysis on the NREL Phase VI turbine [8] recently confirmed the predictability enhancement achieved for the VBM in the present configuration.

$$c_{L\_3D} = c_{L\_2D} + f_L(2\pi(\alpha - \alpha_{c_L=0}) - c_{L\_2D}) \tag{1}$$

$$c_{D\_3D} = c_{D\_2D} + f_D(c_{D\_2D} - c_{D\_2D_{\alpha=0}}) \tag{2}$$

$$f_L = \frac{1}{2\pi}\left[\frac{1.6(c/R)}{0.1267}\frac{1-(c/R)^{1/\left(\Omega r\sqrt{U^2+(\Omega R)^2}\right)}}{1+(c/R)^{1/\left(\Omega r\sqrt{U^2+(\Omega R)^2}\right)}} - 1\right] \tag{3}$$

$$f_D = \frac{1}{2\pi}\left[\frac{1.6(c/R)}{0.1267}\frac{1-(c/R)^{1/\left(2\Omega r\sqrt{U^2+(\Omega R)^2}\right)}}{1+(c/R)^{1/\left(2\Omega r\sqrt{U^2+(\Omega R)^2}\right)}} - 1\right] \tag{4}$$

2.2. CFD setup

As discussed, the VBM model allows the user not to model the blades, which are instead replaced by a single-cell grid layer, within which the model is applied. In the rest of the domain (Fig. 1(b)), the flow field is solved with a conventional RANS approach. In this study, a second-order numerical scheme was used and the turbulence closure was achieved through the k-ω SST model by Menter [14], as originally proposed by [7] and in agreement with previous RANS simulations of HAWTs [8]. The dimensions of the computational domain were set equal to those of the wind tunnel (described in Section 3). Lateral surfaces of the domain were modeled as viscid walls, while velocity inlet and pressure outlet boundaries were used to reproduce the wind tunnel operation. The convergence was achieved as soon as variation of the turbine power output predicted by the VBM was lower than 0.1%.

The mesh was of unstructured type, made of tetrahedral elements in all the domain except for the rotor disk, which was discretized by means of prismatic elements. A dedicated mesh sensitivity analysis was carried out for the single rotor (see Sect. 3). Four meshes (labelled from M1 to M4) were tested, having approximately 400k, 900k, 1800k, and 2900k elements, respectively. Between each mesh, the number of elements inside the fluid disk was doubled, up to mesh M4 which reached the maximum level of discretization intrinsically allowed by the VBM (≈ 8000 elements). Proper refinement was always provided in front of the virtual rotor and along the wake, in order to ensure a low expansion ratio and then a reduced numerical dissipation. The results of the sensitivity analysis (e.g. Fig. 1(c)) were evaluated in terms of velocity difference at each Y position between the wake profiles at different X distances from the rotor. Punctual velocity differences were then reduced into an aggregate parameter through the coefficient of determination (R^2) [8], i.e. the square of the sample correlation coefficient between the observed values at each Y and the observed predictor values, being these the value of the finest mesh M4. It was found that mesh M3 was able to guarantee mesh independent results, being R^2>0.98 for all of the analyzed distances.

3. Selected study cases

The first set of wind tunnel data referred to the famous Blind Tests (BT) by NOWITECH & NORCOWE at the NTNU in Norway. The wind tunnel has a test section 12 m long, 2.7 m wide and about 1.8 m height (Fig. 2(a)). The baseline rotor in BT1 [15] (Fig. 2(c)) was a 3-blade NREL turbine with a S826 airfoil and a diameter D=0.894 m. It has a design tip-speed ratio (TSR) of 6 and the center of the rotor was located at z=0.817 m above the floor level and at 2D distance from the tunnel inlet. Reference wind velocities ranging from 7 to 15 m/s were explored. In BT2 [15], a second rotor (Fig. 2(b)) was placed upstream the first one, at a distance of 3D and with the rotational axis aligned in the wind direction. During the tests, the upwind turbine was maintained at its nominal TSR of 6 while the behavior of the downstream was evaluated for three different TSRs.

In BT3 [15], the same turbines and operating conditions were used but the rotational axes of the rotors were shifted in the y direction of 0.2 m. The second data set was instead taken from [16]. In this study, the same wind turbines and wind tunnel of the Blind Tests were used but in case of a yawed inlet flow. The 1-rotor and the 2-rotor cases were here reproduced at different TSRs and yaw angles for a wind speed of 10 m/s.

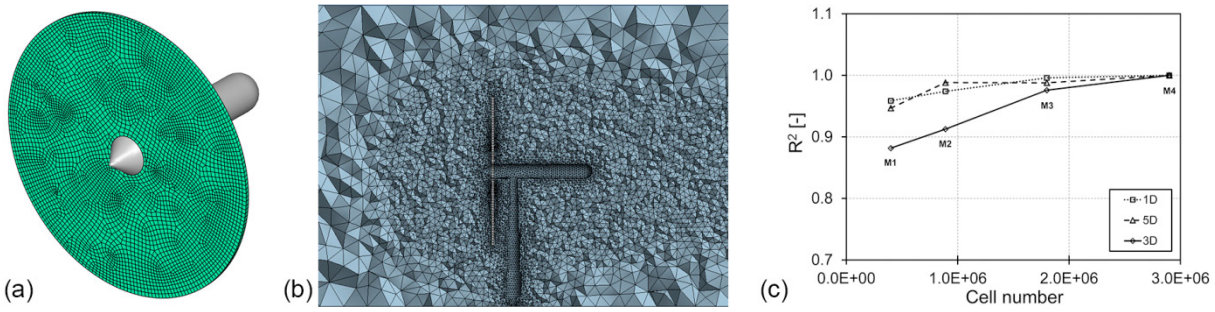

Fig. 1. (a) rotor discretization in the VBM model; (b) mesh around the turbine; (c) mesh sensitivity analysis at TSR=6 in BT1.

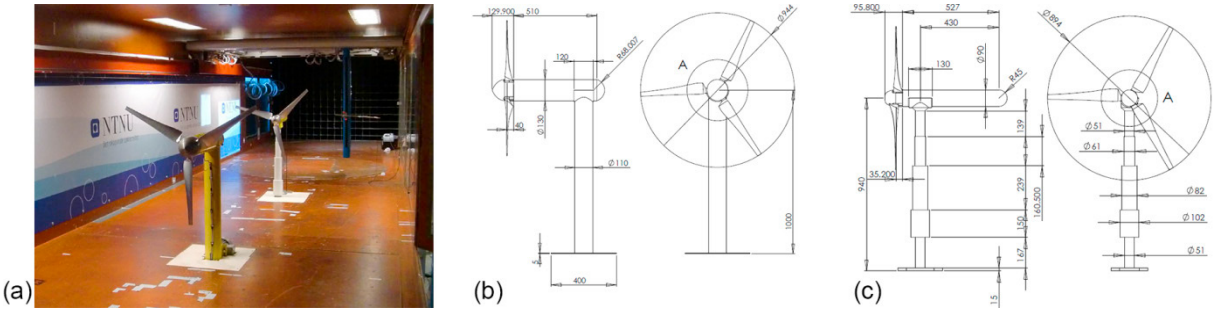

Fig. 2. (a) NTNU wind tunnel; (b) upstream turbine; (c) downstream turbine (also used alone in BT1).

4. Results and discussion

4.1. Blind Test 1 (single rotor)

The assessment of the VBM potential was first carried out on Blind Test (BT) 1 data, which refer to one turbine only tested at various TSRs. Figure 1 collects the main outcomes of the comparison.

In particular, Fig. 1(a) compares the experimental power coefficient curve [15] with that predicted with the VBM: the comparison shows a very good agreement between the two in terms of both the absolute values and the curve shape. A small shift between the curves can be however noticed, in agreement with all the other numerical simulations (with BEM methods or CFD) of the same test case. The reasons of such a discrepancy can be hypothesized upon examination of Fig. 3(b) and Fig. 3(c), which report (in terms of dimensionless velocity, U/U_0) the near and far wake profiles, respectively, at the rated tip-speed ratio of TSR=6.

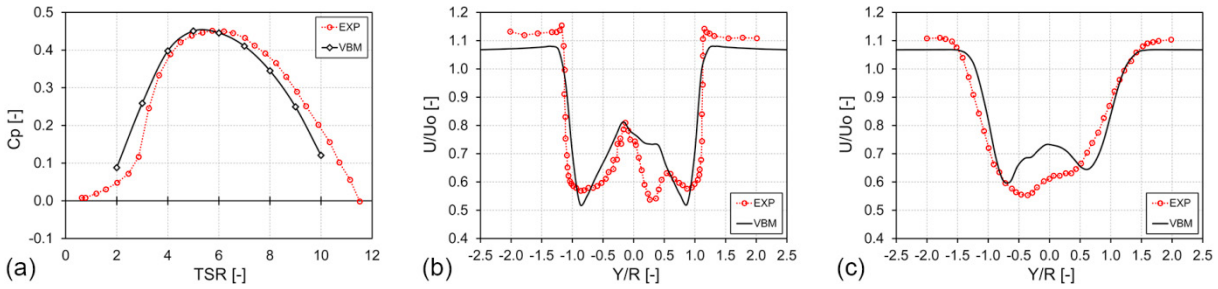

Fig. 3. Results of BT1 - (a) *Cp* vs. TSR; profiles of: (b) near wake (1D) and (c) far wake (5D) @ TSR=6.

It is indeed apparent that numerical simulations predicted a lower wind speed within the tunnel in reason of an attended blockage effect (induced by the presence of the turbine) lower than that estimated from experiments. This conclusion is again in agreement with the conclusions drawn by other researchers on the same test case [15].

Overall, however, the VBM was able to quite reliably predict the shape of the near wake (1D downstream) and the far wake (5D), where a discrepancy is only noticeable in the center of the wake, suggesting a longer extension of the wake in experiments with respect to numerical simulations.

4.2. Blind Test 2 (two aligned rotors)

In BT2, the aerodynamic performance of the same turbine was studied at different TSRs while working in the wake of an upstream additional rotor operating at its nominal TSR=6. According to previous BT, Fig. 4(a) first reports the comparison between experimental power coefficients [15] and VBM estimations at those specific TSRs for which detailed wake measurements were available. Once again, the agreement between experiments and VBM data is particularly promising despite the quite simplified theoretical approach at the basis of the model.

An even better agreement was noted in terms of wake profile description at all the three investigated TSRs of the downstream turbine. For brevity reasons, the only comparisons at the nominal working condition of TSR=4.0 are here reported for the near wake (1D – Fig. 4(b)) and the far wake (4D – Fig. 4(c)), respectively. Both comparisons show an impressive matching between experiments and simulations, even better than that obtained for the single rotor in BT1, possibly due to the fact that the downstream rotor is less loaded in comparison to the upstream one in reason of the lower oncoming wind (Fig. 5) [8]. In these conditions, some aerodynamic effects like the wake rotation, the tip effects and the flow-nacelle interaction – which are typically hard to properly model with low-fidelity theories like the BEM – have a lower impact on the rotor performance.

The mismatch on the prediction of the induced blockage around the downstream rotor seems also to be reduced in comparison to the upstream turbine, suggesting (see Fig. 5) that the major impact is due to the first interaction between the flow and the first rotor, possibly connected to inlet flow distortions in the wind tunnel.

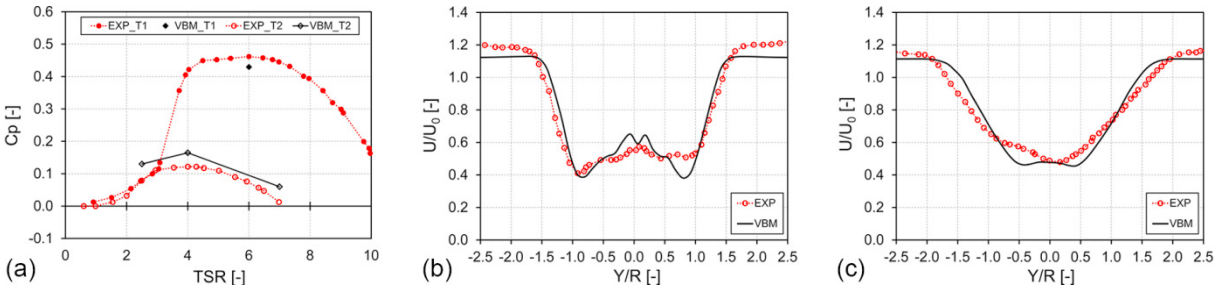

Fig. 4. Results of BT2 - (a) *Cp* vs. TSR for the two turbines; (b) near wake (1D) and (c) far wake (4D) @ TSR_T2=4.

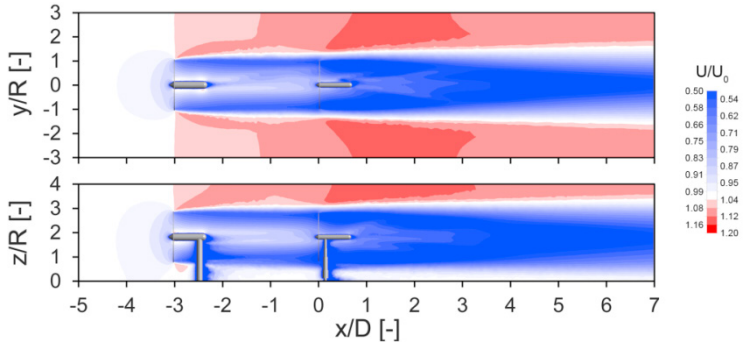

Fig. 5. Velocity contours in BT2 @ TSR_T2=4: (up) *xy* plane; (down) *xz* plane.

4.3. Blind Test 3 (two misaligned rotors)

The same analyses of BT2 were repeated in BT3 in case the downstream rotor is shifted laterally with respect to the upstream one; this configuration is indeed typical of wind turbine clusters. Again, good agreement is first noticeable in Fig. 6(a) in terms of power coefficient vs. TSR. Focusing on wake profiles, the robustness of VBM predictions was again confirmed at all the three tested TSRs. For brevity reasons, the only comparisons at the nominal working condition of TSR=4.75 are here reported for the near wake (1D – Fig. 6(b)) and the far wake (3D – Fig. 6(c)), respectively. Despite the complexity of the flow field, the main aerodynamic phenomena are clearly distinguishable in the wake profile through simulations, again confirming the good accuracy of the VBM. As expectable based on the turbine layout (see for example Fig. 7), simulations suggest the presence of a quite high blockage effect in experiments, testified by the lateral velocity profiles in Fig. 6(b) and Fig. 6(c).

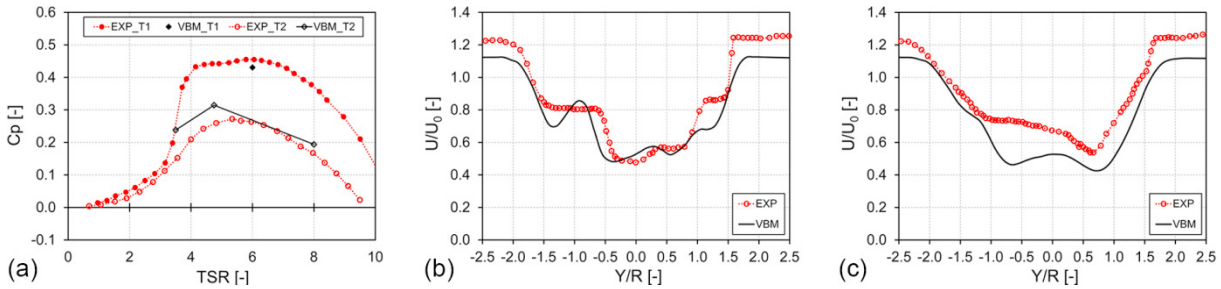

Fig. 6. Results of BT3 - (a) *Cp* vs. TSR for the two turbines; (b) near wake (1D) and (c) far wake (3D) @ TSR_T2=4.75.

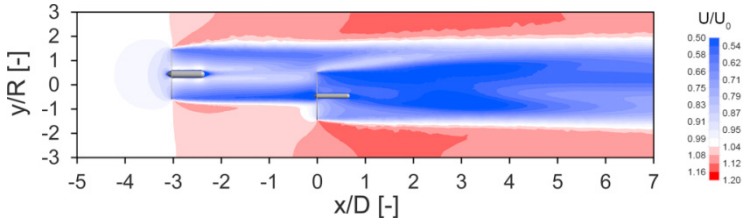

Fig. 7. Velocity contours in BT3 @ TSR_T2=4.75: *xy* plane.

4.4. Yawed flow tests

The final cases for the validation of the VBM were represented by the wind tunnel tests carried out by Andresen [16] on the same turbines within the same tunnel of the NOWITECH & NORCOWE campaigns. Performance and wake measurements were first performed on a single turbine, which was rotated to induce a yaw angle between the incoming wind and the turbine axis. Then (Fig. 8(a)), the effects on the downstream rotor were analyzed.

The *Cp* variation of the single turbine in yawed flow (Fig. 8(b)) accurately followed the typical trend already described by [12] and dependent on $\cos^3(\gamma)$. If compared to VBM predictions, good agreement was also appreciated between experiments and simulations for the wake profiles (e.g. Fig. 8(c)), testifying the accuracy of the VBM even in case of a misaligned flow. This feature of the model makes it particularly promising for all those applications which are characterized by misaligned flows (e.g. the urban environment [12]). The progressive reduction of the energy extracted by the turbine as a function of the yaw angle is well depicted by the velocity contours reported in Fig. 9 for skew angles of 10°, 30° and 50°, respectively. The intensity of the turbine wake is indeed progressively reduced, becoming also strongly affected by the separation phenomena occurring in the surroundings of the nacelle.

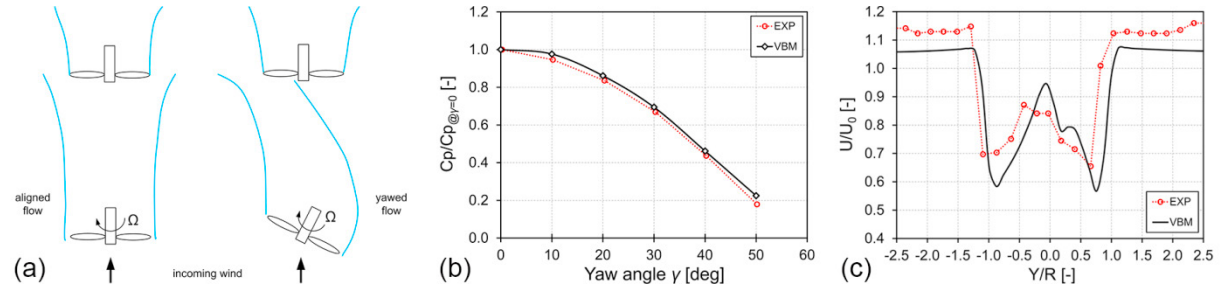

Fig. 8. Test results in yawed flow: (a) qualitative wake behavior in yawed flow; (b) *Cp* variation as a function of the yaw angle; (c) example of wake profile description in yawed flow: near wake (1D) for γ=20°.

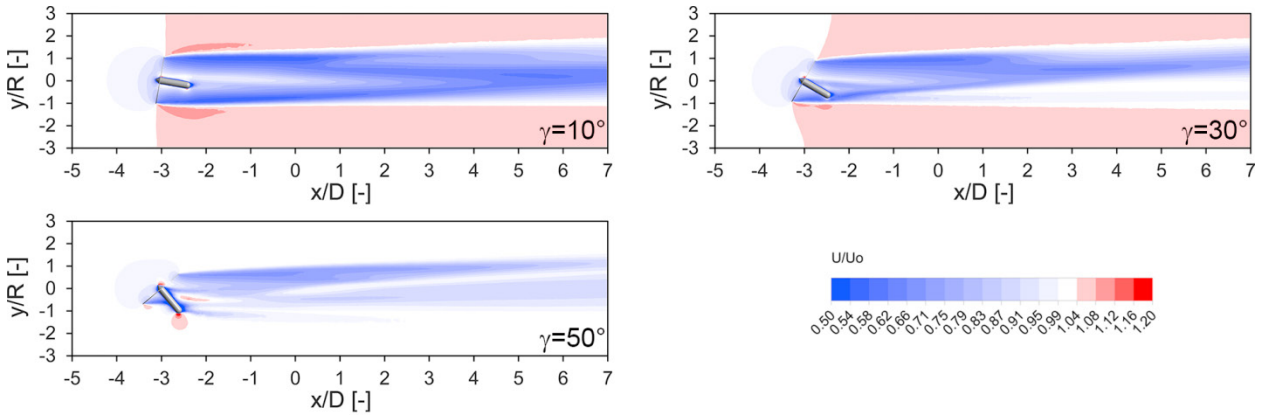

Fig. 9. Test results in yawed flow @ TSR=6: velocity contours at yaw angles of 10°, 30° and 50°, respectively.

Finally, the 2-turbine case was analyzed. Figure 10(a) first compares the power coefficient curves of the downstream rotor as a function of TSR for three relevant yaw angles of the upstream rotor of 0°, 20° and 40°, respectively. Again, sound agreement was found between experiments and simulations, with a correct description of the *Cp* values, the curve shape and the position of the peak efficiency. As attended, the performance of the downstream rotor is now enhanced for increasing yaw angles, in contrast with the former results of BT2. As clearly shown by Fig. 10(b), as soon as *γ* increases, the downstream rotor indeed works with a more energized flow leaving the less-efficient upstream rotor. The good handling of the VBM model of the wake interaction shown by these tests and by blind tests 2 and 3 corroborated the suitability of the model itself for wind park or array studies.

5. Conclusions

In the present study, the potential of the Virtual Blade Model (VBM) for ANSYS® FLUENT®, originally conceived for helicopter blades, in the performance analysis and the description of wind turbine wakes was assessed by comparing numerical predictions with several sets of wind tunnel data, many of which are part of the famous NOWITECH-NORCOWE blind tests for horizontal axis wind turbines.

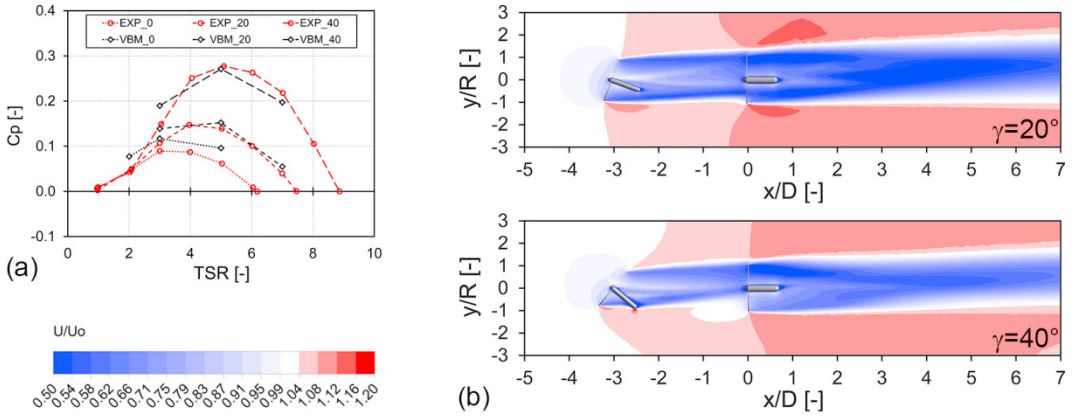

Fig. 10. Test results in yawed flow for two turbines: (a) *Cp* vs. TSR for the downstream turbine; (b) velocity contours at yaw angles of 20° and 40°, respectively @ TSR_T2=5.

The test cases included: 1) a single turbine; 2) an array of two turbines with one rotor working in the wake of the other one; 3) an array of two staggered rotors; 4) several configurations of rotors working in yawed-flow.

Overall, the model – if applied with the custom modifications and the numerical framework presented in the paper – was able to properly model the main features of the wake of all the turbines, in case of both a single rotor or two rotors. A reliable estimation of the turbine performance was also provided in all the study cases. In particular, sound agreement was found also for the tests in yawed flow, confirming the prospects of this method in wind energy applications, even in case of non-conventional siting problems like, for example, the urban environment.

Acknowledgements

The activity presented in the paper is part of the grant assigned to Dr. Francesco Balduzzi by the *Fondazione Cassa di Risparmio di Firenze*, which is sincerely acknowledged for its invaluable effort is sustaining the university research. Thanks are due to Prof. Ennio Antonio Carnevale of the University of Florence for supporting this activity.

References

[1] GWEC. Global Wind Report 2016. Tech. rep., 2016.
[2] Sanderse B. Aerodynamics of Wind Turbine Wakes,. Tech. rep., ECN-E–09-016, 2009.
[3] Göçmen T, van der Laan P, Réthoré P-E, Peña Diaz A., Larsen GC, Ott S. Wind turbine wake models developed at the technical university of Denmark: A review. Renewable and Sustainable Energy Reviews 2016; 60(July 2016): 752-769.
[4] Sørensen JN. Wake Modelling Status and Perspectives. Keynote lecture at the HPC Core Workshop, Lancaster (UK), 7-8 April 2016.
[5] Crespo A, Hernandez J, Frandsen S. Survey of Modeling Methods for Wind Turbine Wakes and Wind Farms. Wind Energy 1999; 2: 1-24.
[6] Martınez-Tossas LA, Leonardi S. Wind Turbine Modeling for Computational Fluid Dynamics December 2010 - December 2012. Tech. rep., NREL/SR-5000-55054, 2013.
[7] Javaherchi Mozafari AT. Numerical Modeling of Tidal Turbines: Methodology Development and Potential Physical Environmental Effects. MSc Thesis in Mechanical Engineering, University of Washington (USA), 2010.
[8] Bianchini A, Balduzzi F, Gentiluomo D, Ferrara G, Ferrari L. Comparative analysis of different numerical techniques to analyze the wake of a wind turbine. Proc. of the ASME Turbo Expo 2017, Charlotte (NC), USA, June 25-30, 2017.
[9] Laith Z, Rajagopalan R. Navier-Stokes calculations of rotor-airframe interaction in forward flight. Journal of the American Helicopter Society 1995; 40(2): 57-67.
[10] Burton T, Sharpe D, Jenkins N, Bossanyi E. Wind Energy Handbook. J. Wiley & sons Ltd, Oxford (UK), 2001.
[11] Cerisola A. Numerical Analysis of Tidal Turbines using Virtual Blade Model and Single Rotating Reference Frame. Tech. rep., University of Washington, 2012, http://depts.washington.edu/fluidlab/reports/a_cerisola_rapport.pdf, last access 05/10/2016.
[12] Bianchi S, Bianchini A, Ferrara G, Ferrari, L. Small wind turbines in the built environment: influence of flow inclination on the potential energy yield. Journal of Turbomachinery 2004; 136(4): 1-9.
[13] Du Z, Selig MS. A 3-D stall-delay model for horizontal axis wind turbines performance prediction. Proc. of the 1998 ASME Wind Energy Symposium, January 12-15 1998, Reno, Nevada, USA, paper no AIAA-98-0021.
[14] Menter F. Two-equation Turbulence-models for Engineering Applications. AIAA Journal 1994; 32(8): 1598–1605.
[15] Krogstad PA, Sætran L. Wind turbine wake interactions; results from blind tests. J. of Physics: Conference Series 2015; 625: 012043-1-21.
[16] Andresen B. Wake behind a wind turbine operating in yaw. MSc thesis, NTNU, Trondheim, Norway, 2013.